Supporting Information

Cationic Copolymerization of Isosorbide Towards Value-added Poly(vinyl ethers)

Robert J. Kieber III, Cuneyt Ozkardes, Natalie Sanchez, and Justin G. Kennemur[a]*

[a] Department of Chemistry and Biochemistry, Florida State University, Tallahassee, FL 32303 USA

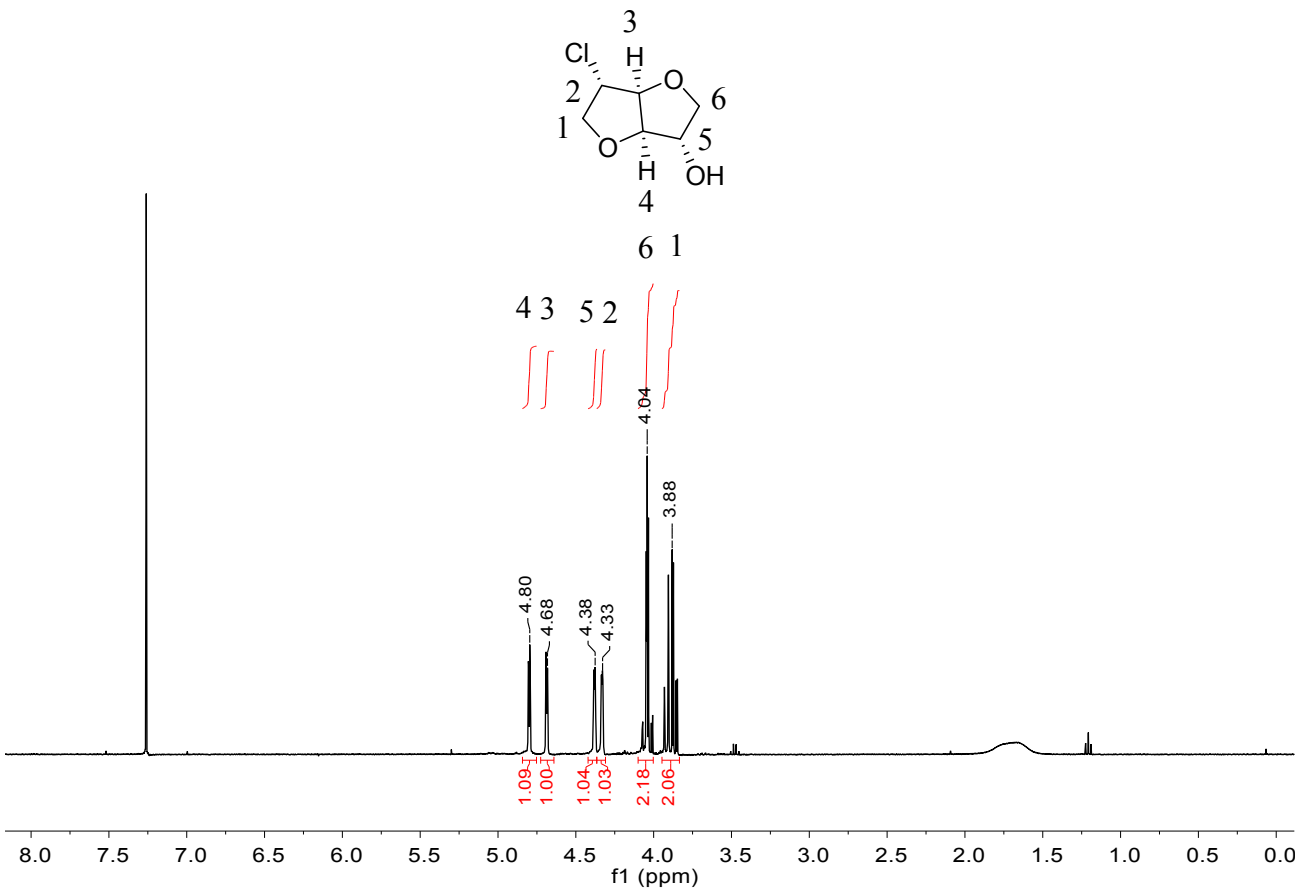

Figure S1: ^{1}H NMR of (3S,3aR,6S,6aS)-6-chlorohexahydrofuro[3,2-b]furan-3-ol (**1**) (600 MHz, $CDCl_3$, 25 °C)

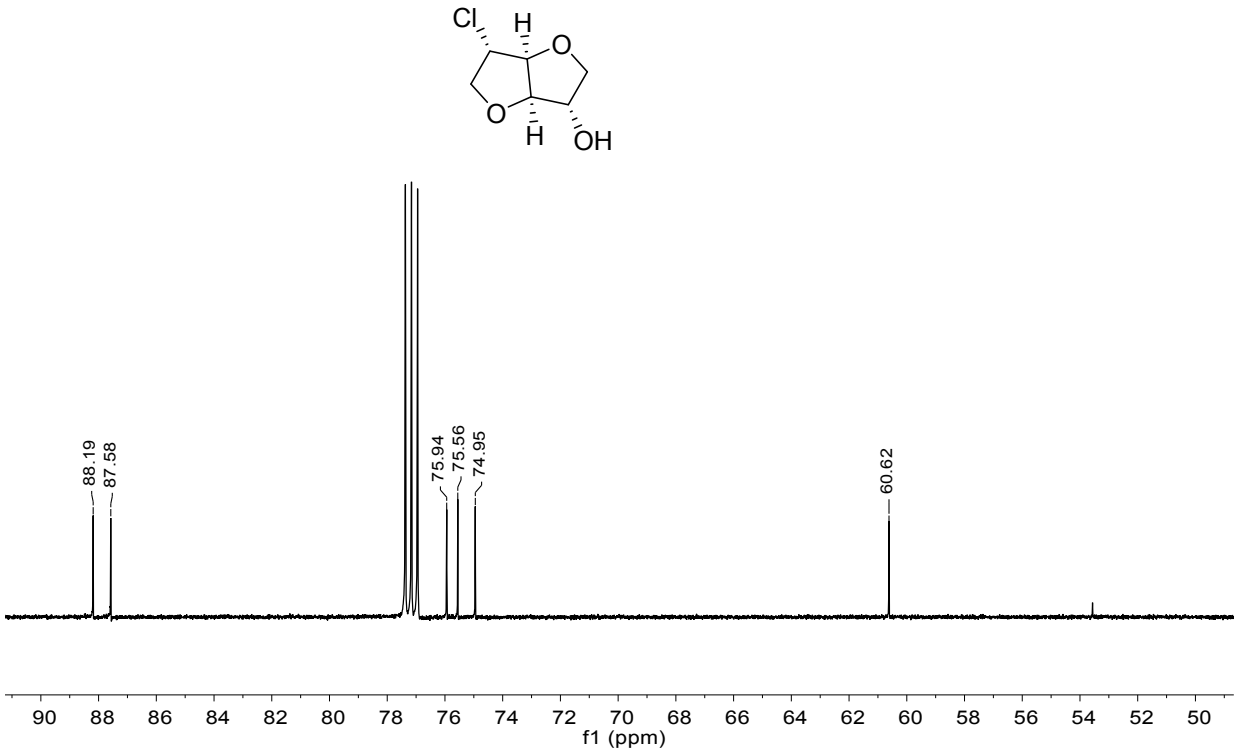

Figure S2: ^{13}C NMR of (**1**) (151 MHz, $CDCl_3$, 25 °C)

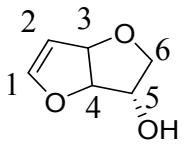

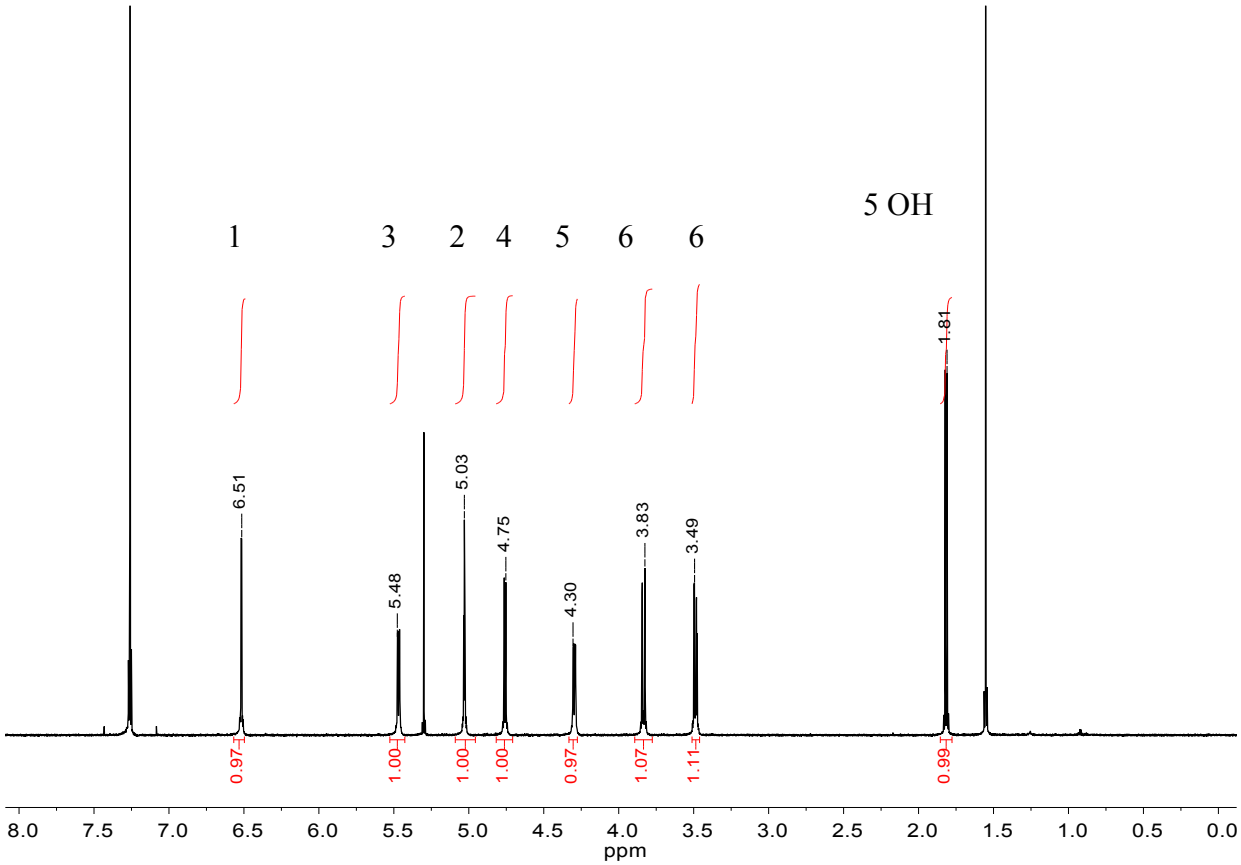

Figure S3: ^{1}H NMR of (3S,3aR,6aR)-2,3,3a,6a-tetrahydrofuro[3,2-b]furan-3-ol (**2**) (600 MHz, $CDCl_3$, 25 °C)

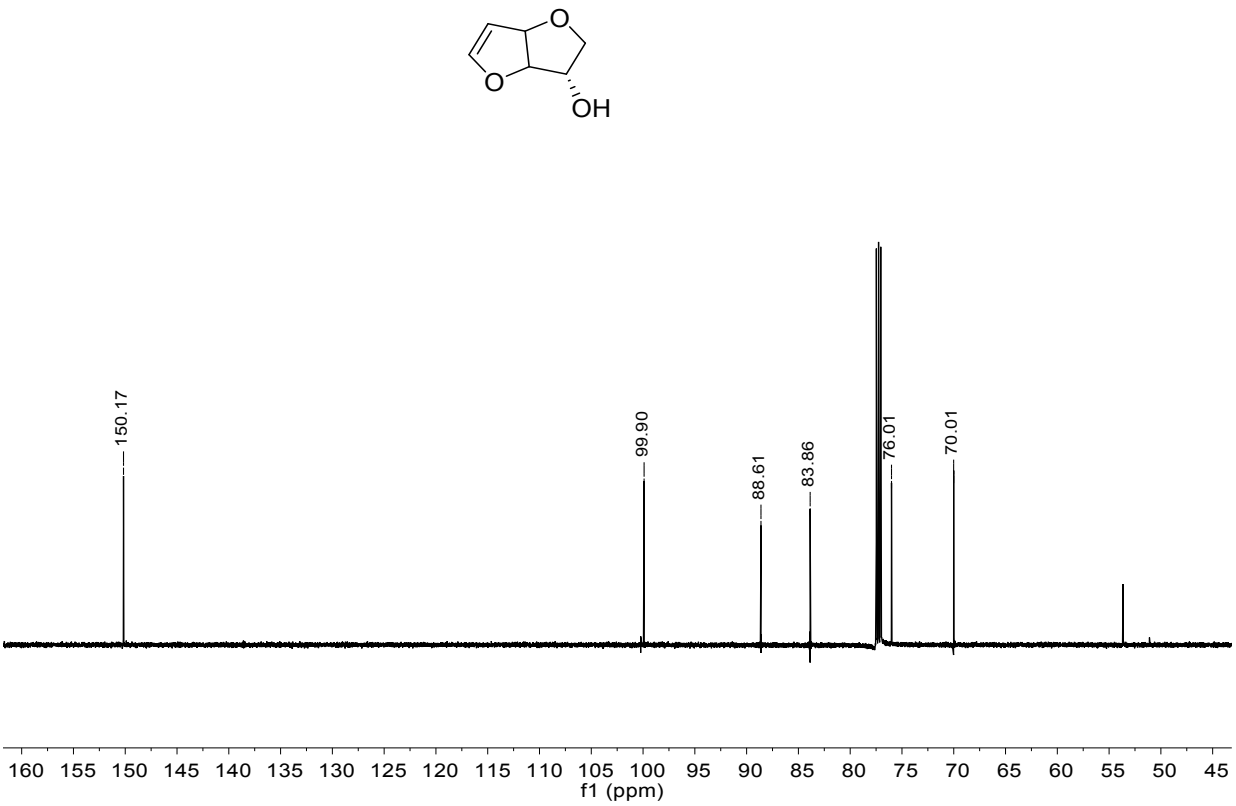

Figure S4: ^{13}C NMR of (**2**) (151 MHz, $CDCl_3$, 25 °C)

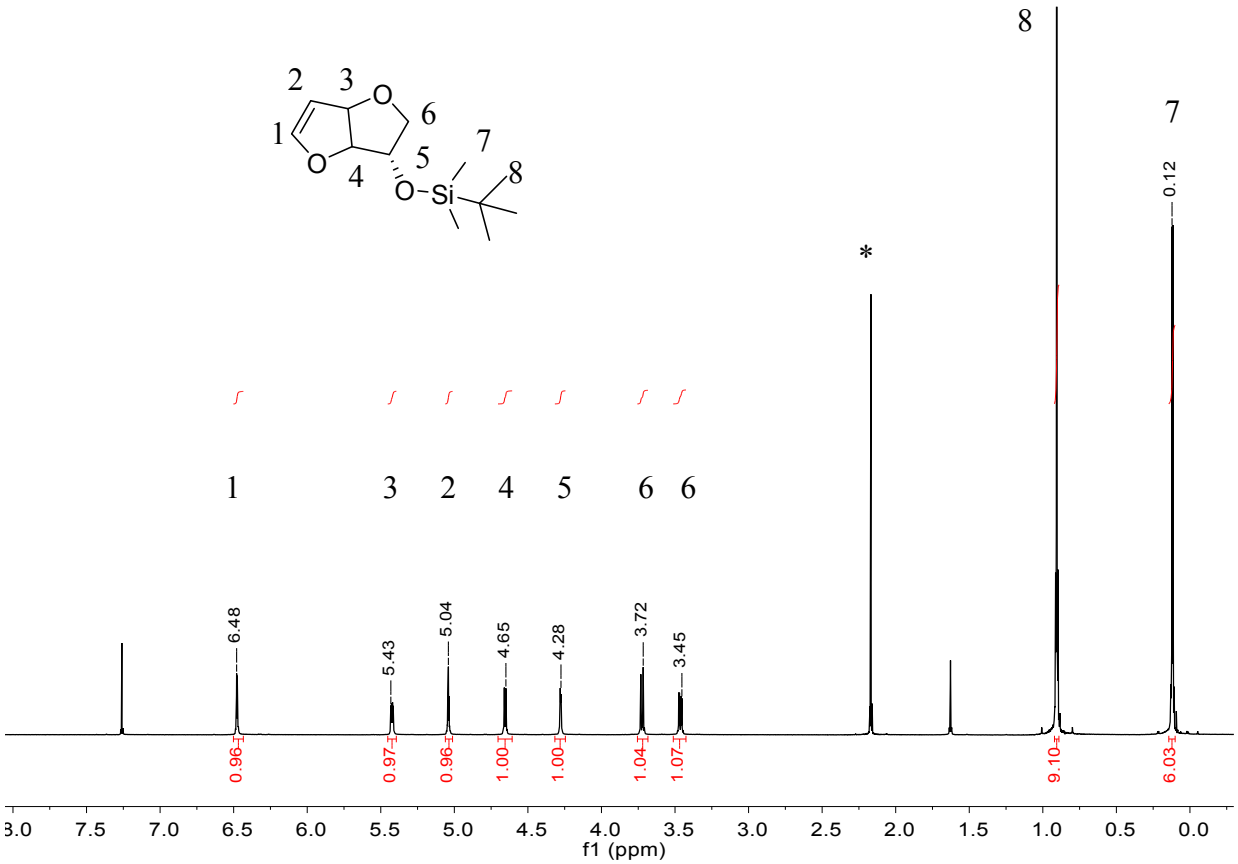

Figure S5: ^{1}H NMR of tert-butyldimethyl(((3S,3aS,6aR)-2,3,3a,6a-tetrahydrofuro[3,2-b]furan-3-yl)oxy)silane (**3**) (600 MHz, $CDCl_3$, 25 °C). Asterisk (*) denotes acetone peak

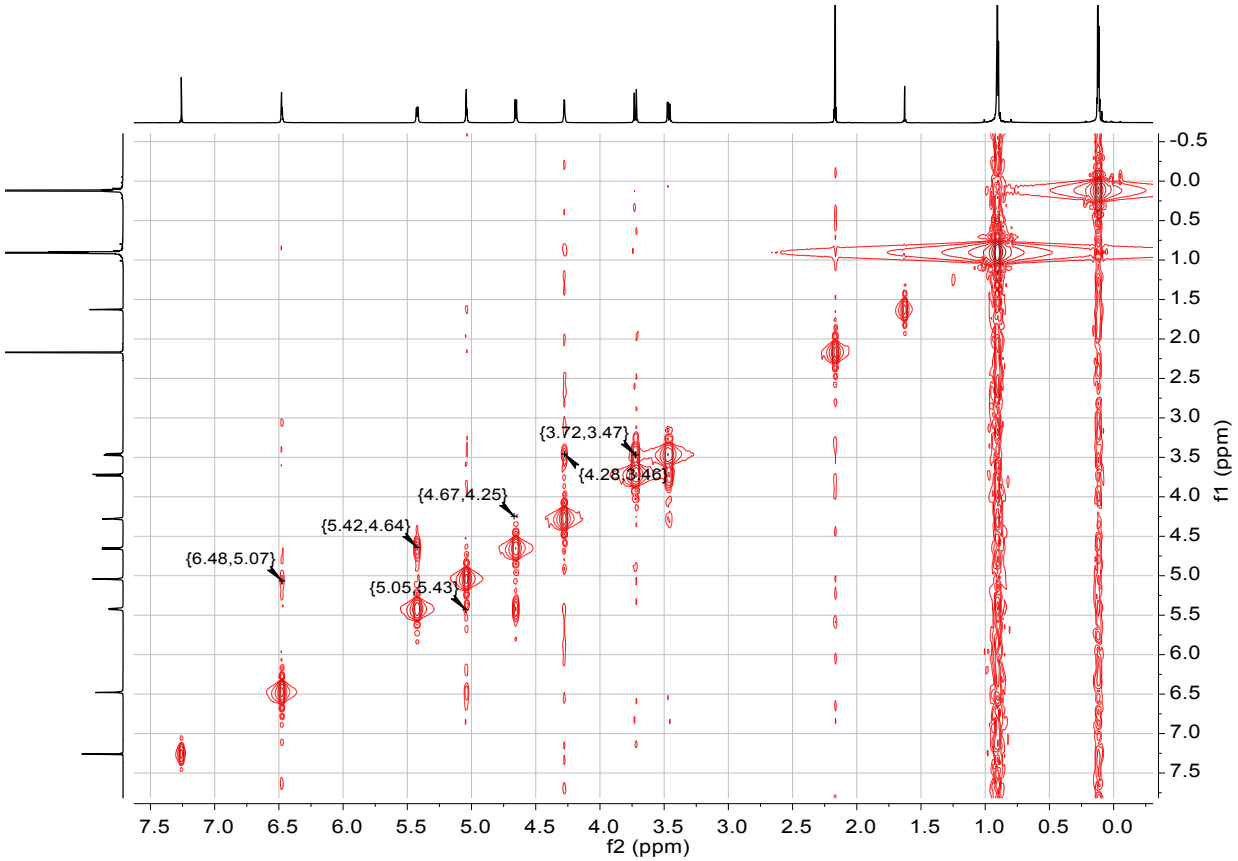

Figure S6: ^{1}H-^{1}H COSY of **3** (600 MHz, $CDCl_3$, 25 °C)

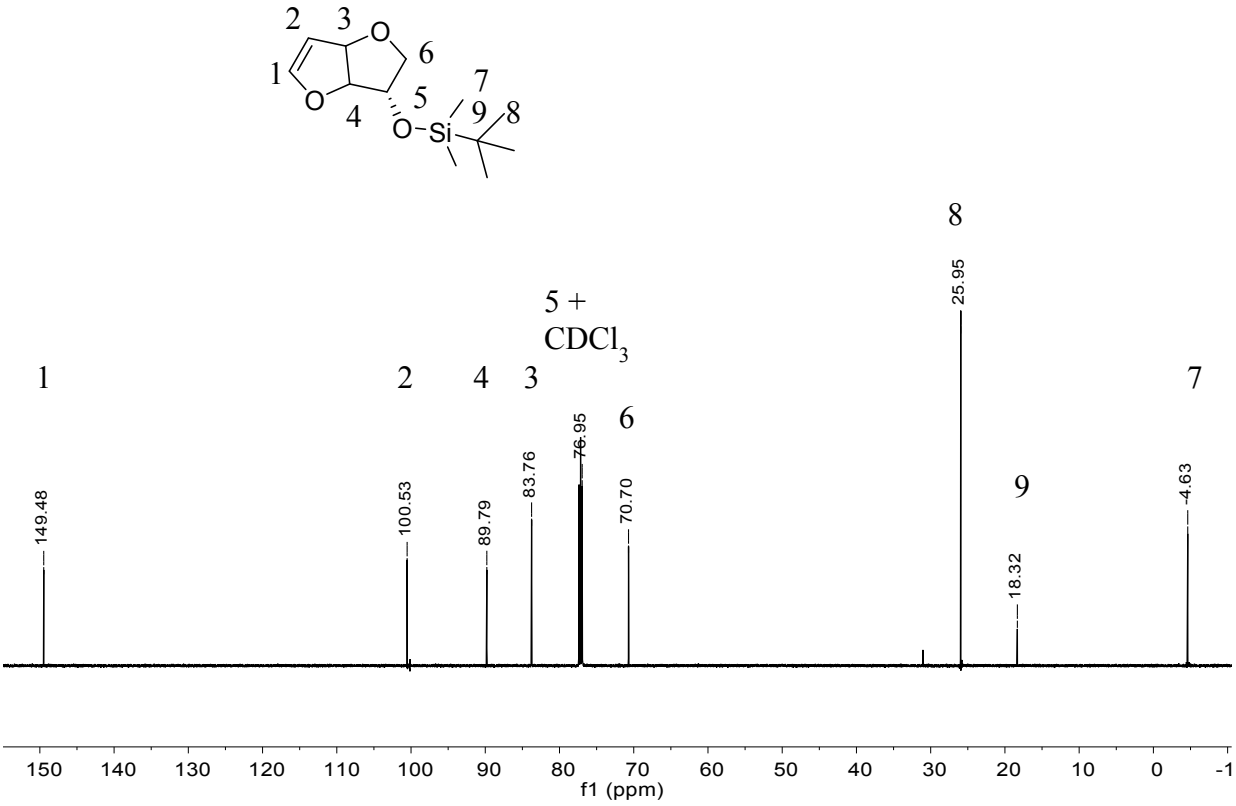

Figure S7: ^{13}C NMR of **3** (151 MHz, $CDCl_3$, 25 °C)

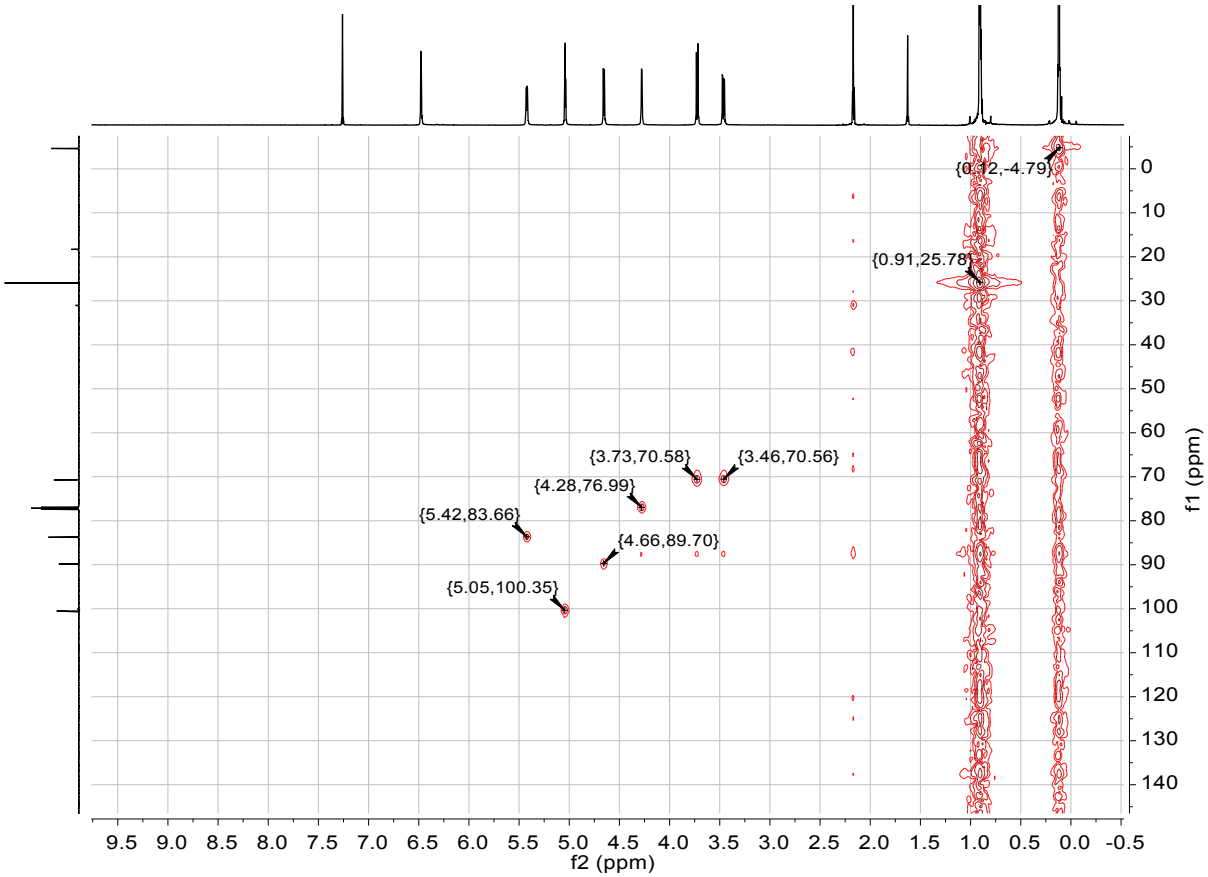

Figure S8: ^{1}H-^{13}C HMQC of **3** (600 MHz, 151 MHz, $CDCl_3$, 25 °C)

Scheme S1: Synthesis of RAFT agent, *S*-1-isobutoxylethyl-*S*′-ethyl trithiocarbonate (**4**)

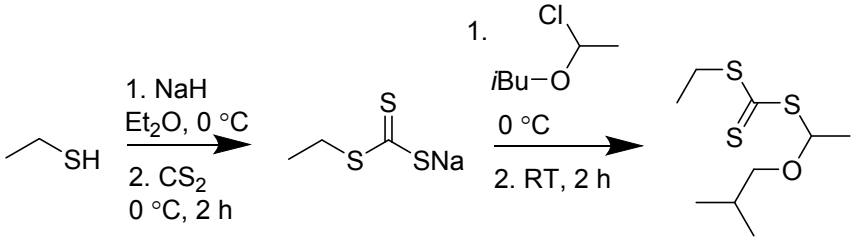

4

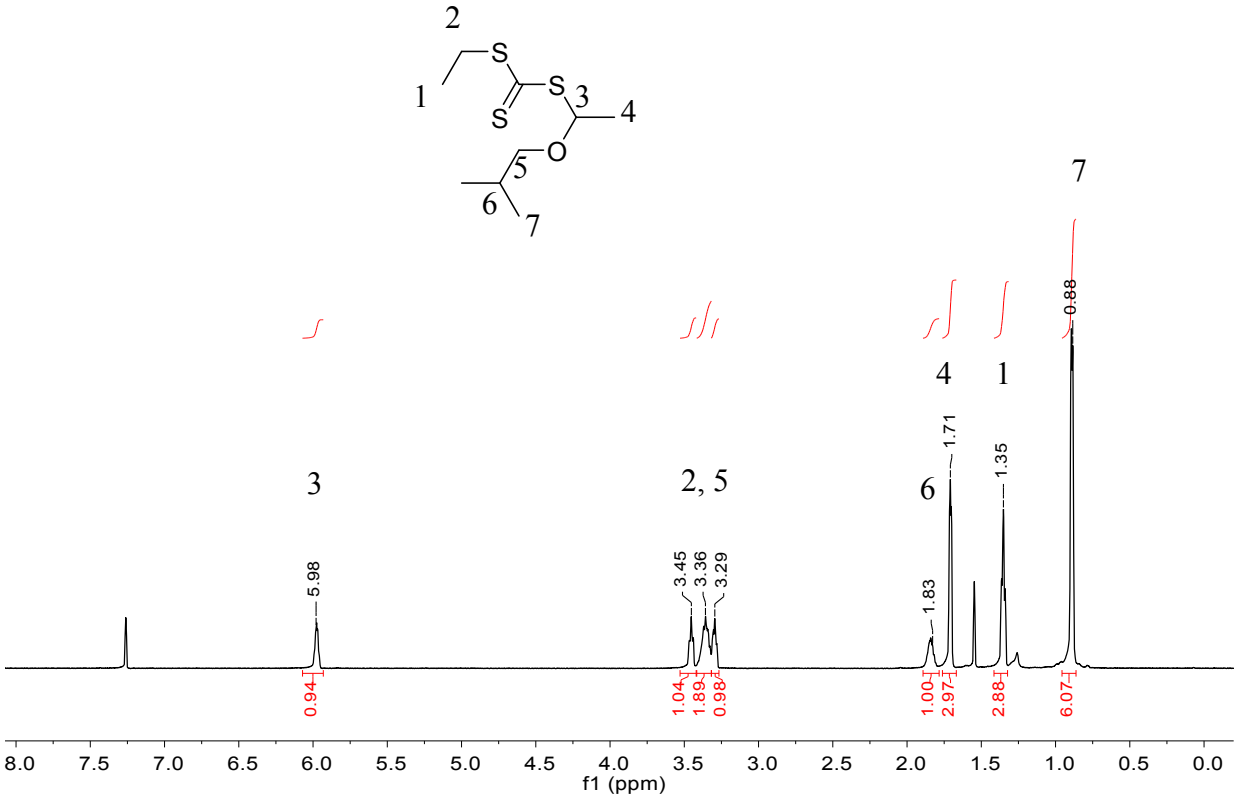

Figure S9: ^{1}H NMR of **4** (600 MHz, $CDCl_3$, 25 °C)

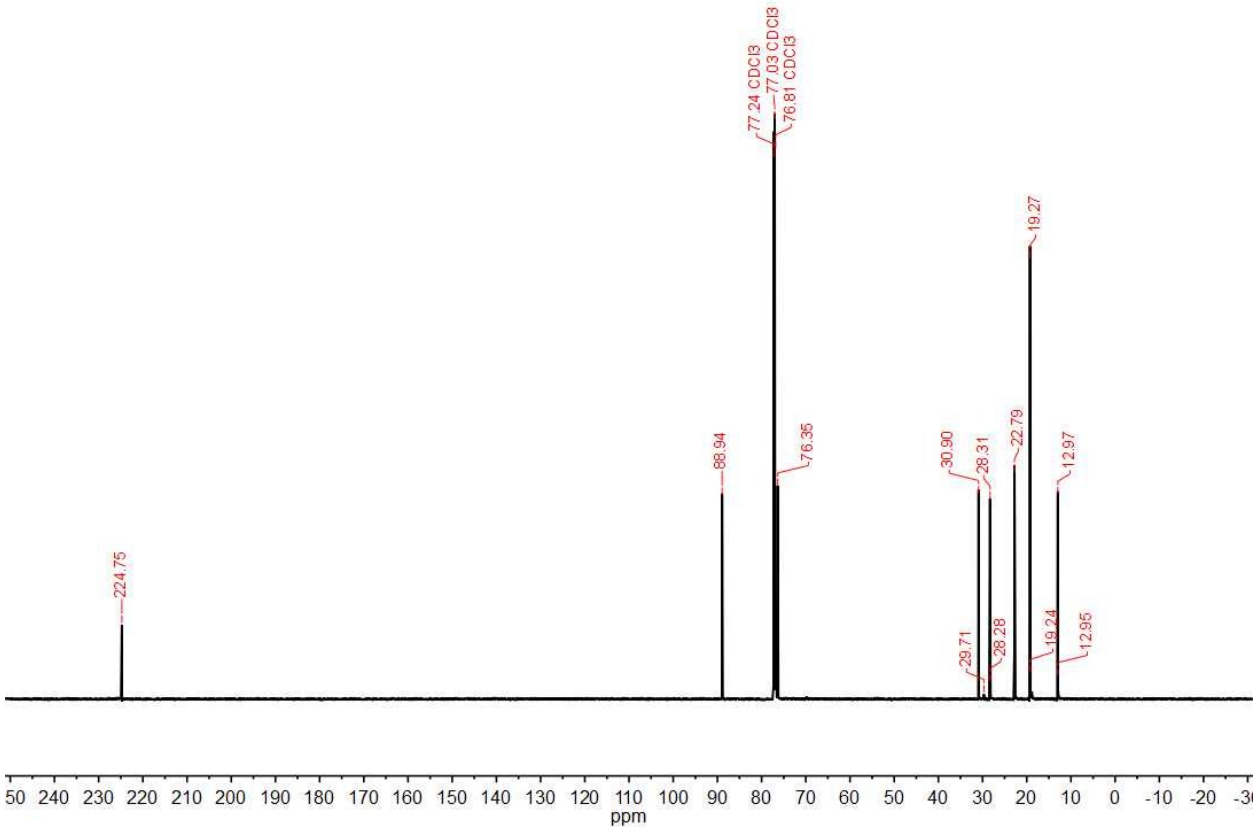

Figure S10: ^{13}C NMR of **4** (151 MHz, $CDCl_3$, 25 °C)

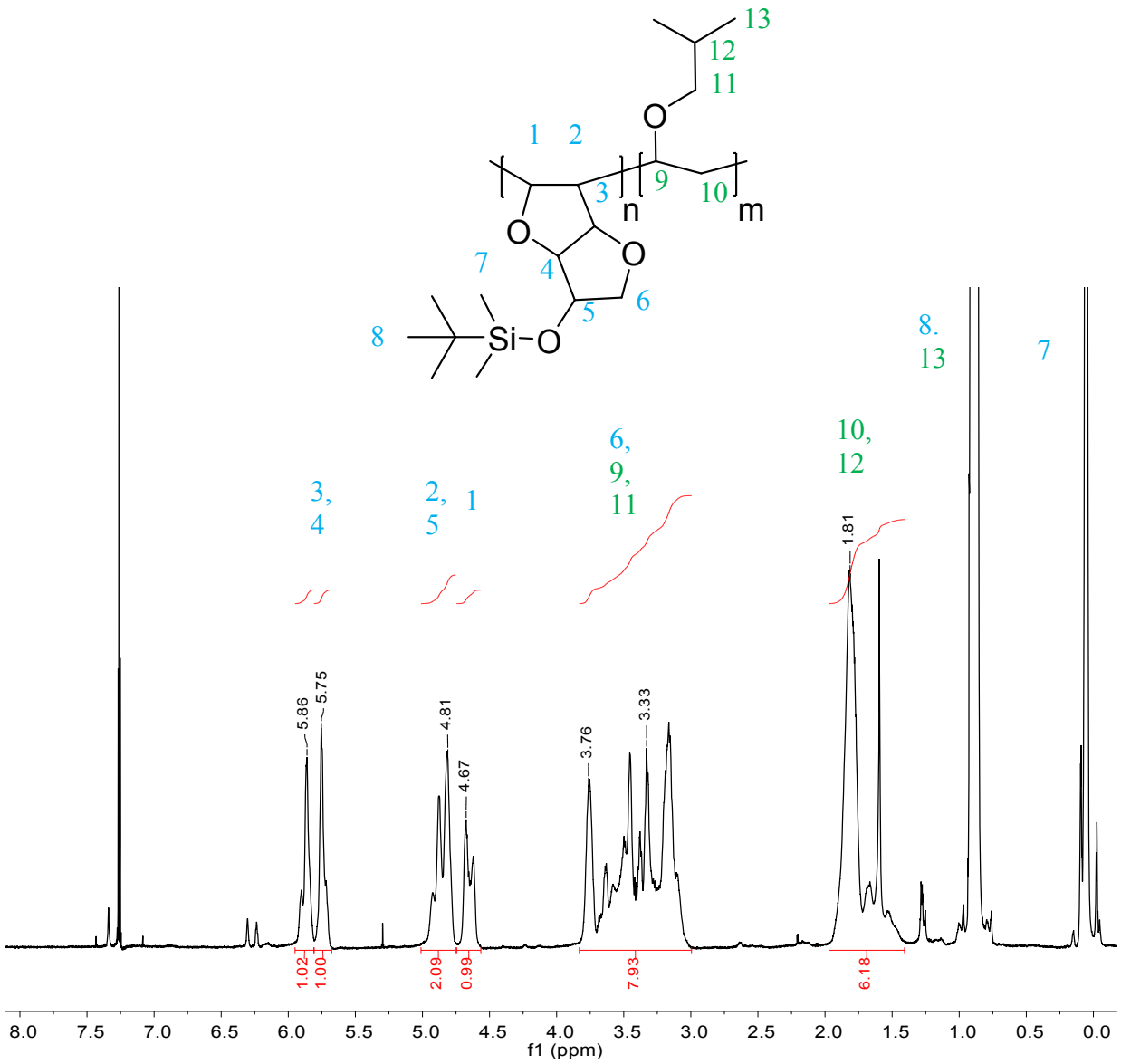

Figure S11: ^{1}H NMR of P33 (600 MHz, $CDCl_3$, 25 °C)

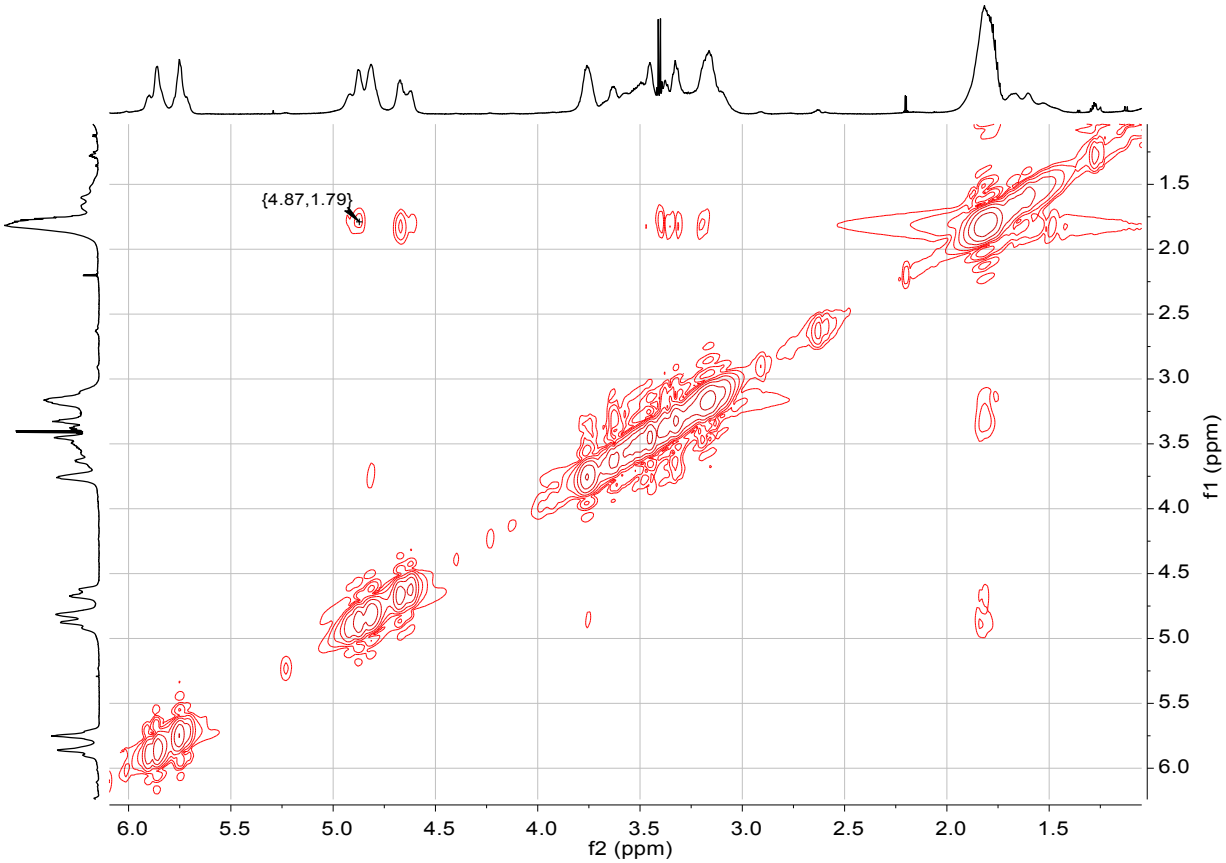

Figure S12: ^{1}H-^{1}H COSY of P33 (600 MHz, $CDCl_3$, 25 °C).

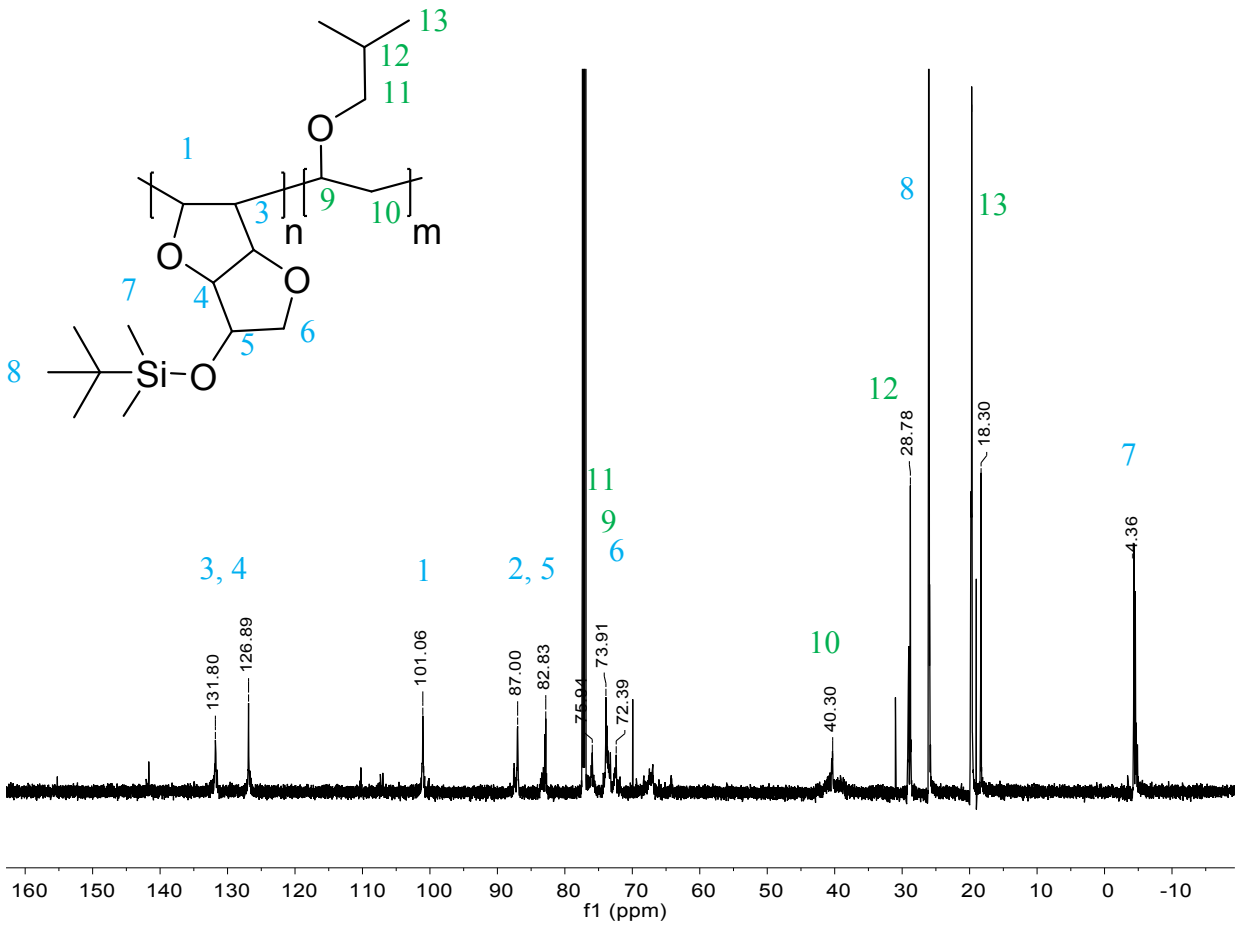

Figure S13: ^{13}C NMR of P33 (151 MHz, $CDCl_3$, 25 °C)

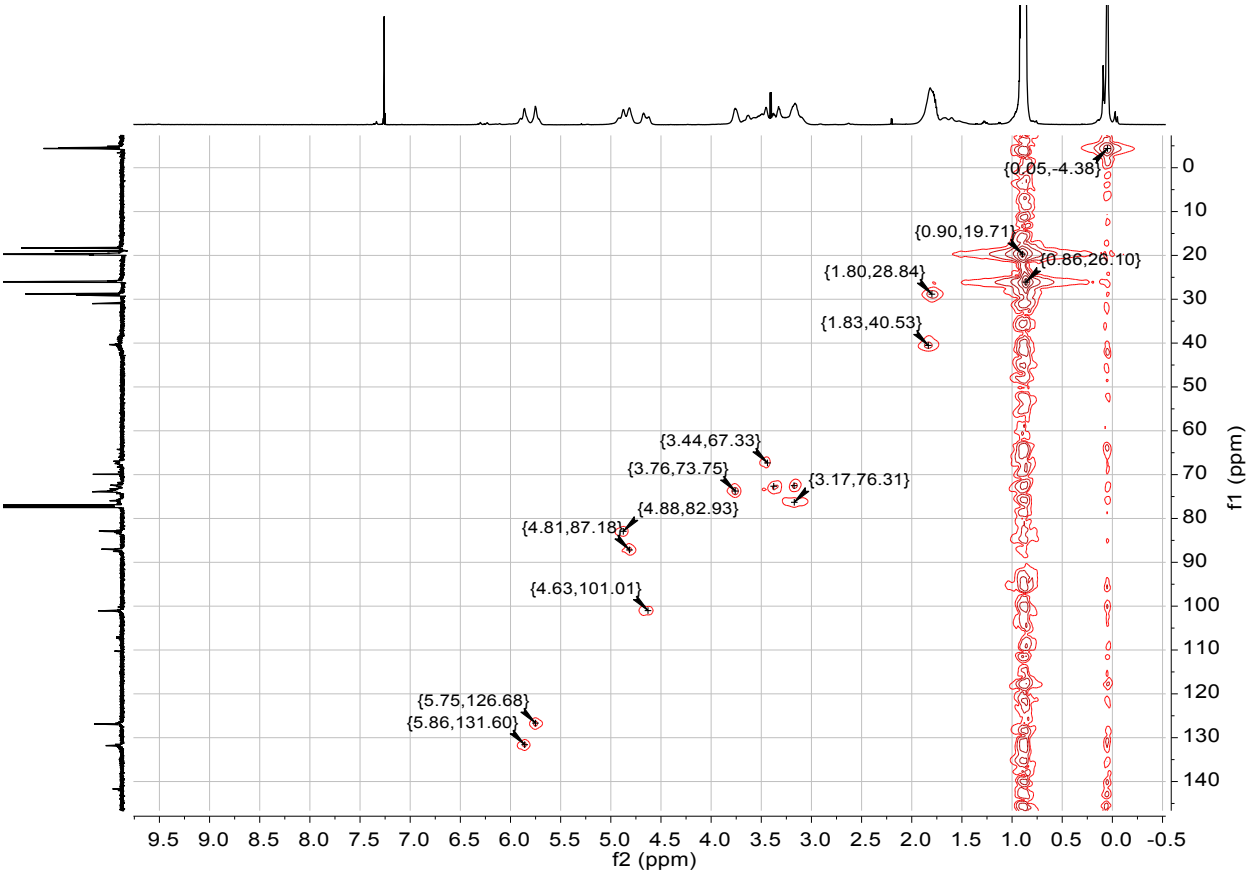

Figure S14: ^{1}H-^{13}C HMQC NMR of P33 (600 MHz, 151 MHz, $CDCl_3$, 25 °C)

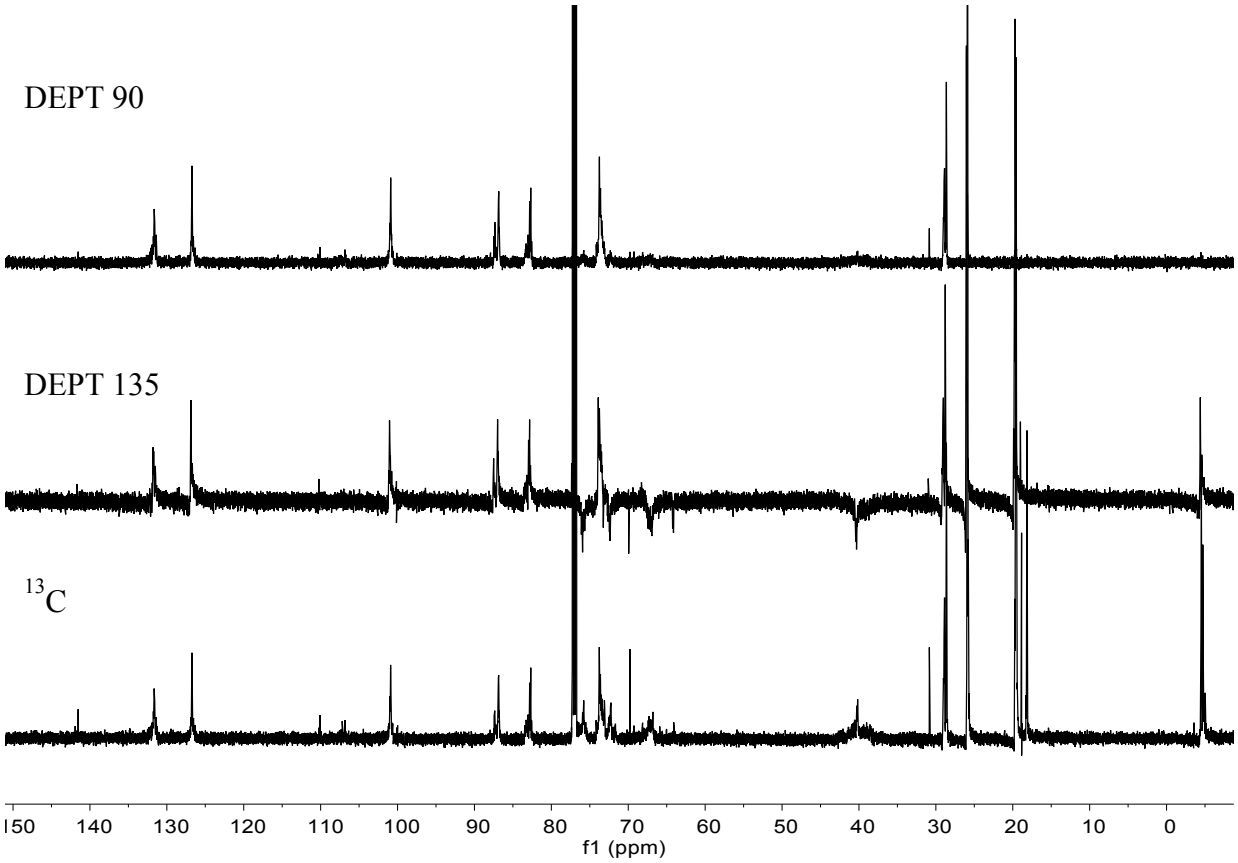

Figure S15: DEPT 90 (top), DEPT 135 (middle) and ^{13}C NMR overlay P33 (151 MHz, $CDCl_3$, 25 °C)

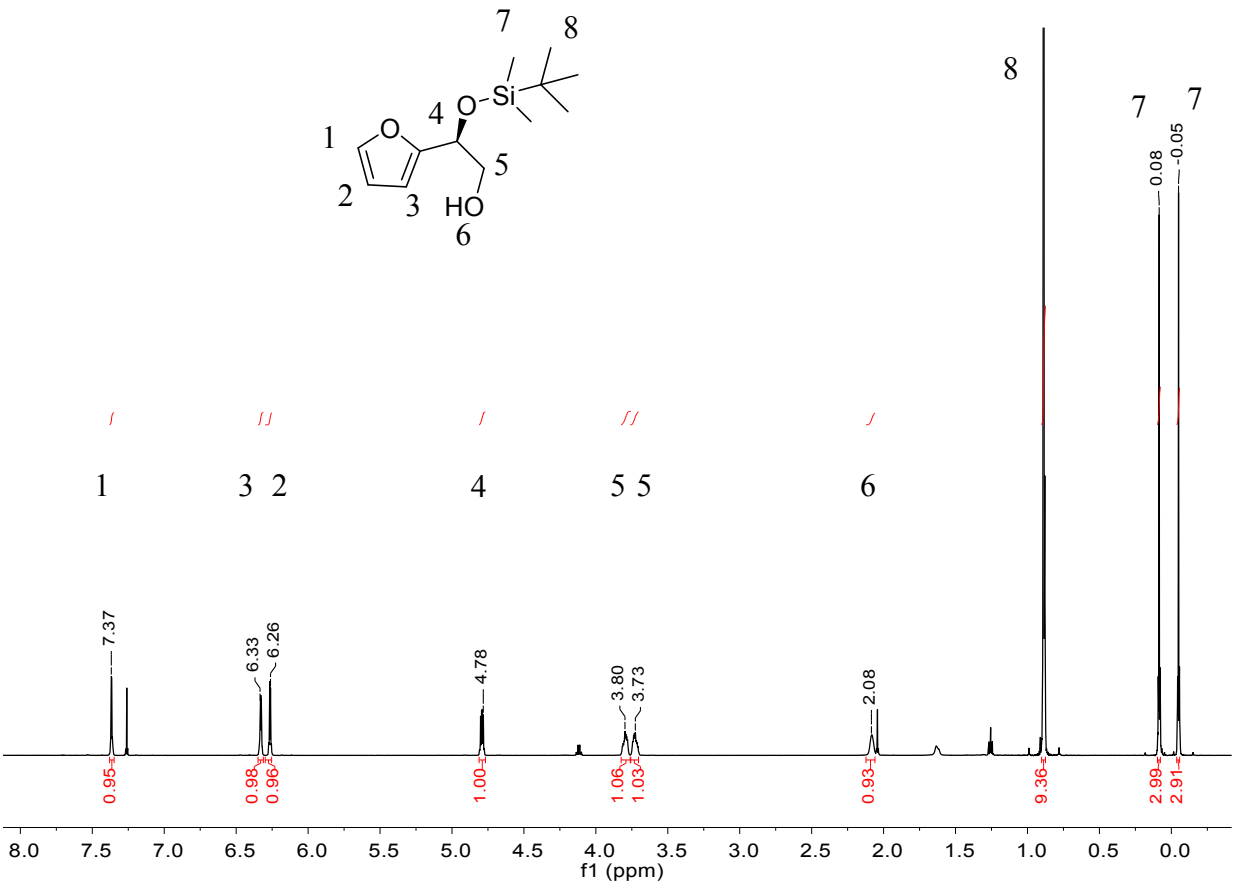

Figure S16: ^{1}H NMR of (*S*)-2-((tert-butyldimethylsilyl)oxy)-2-(furan-2-yl)ethan-1-ol (**5**) (600 MHz, $CDCl_3$, 25 °C)

Scheme S2: Ring opening of **3** using pyridinium *p*-toluenesulfonate (PTSA) and proposed mechanism[1-2]

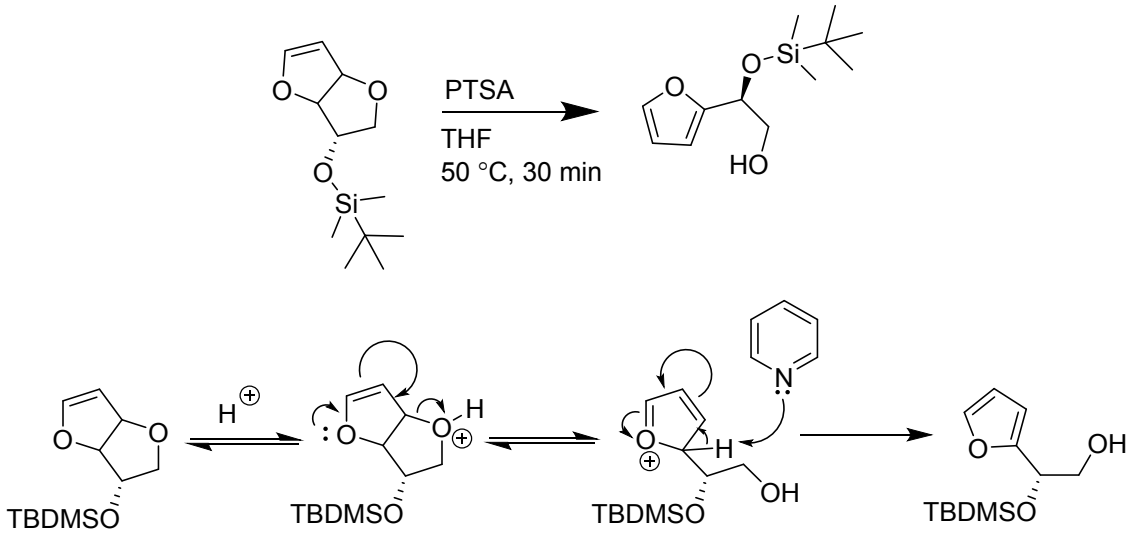

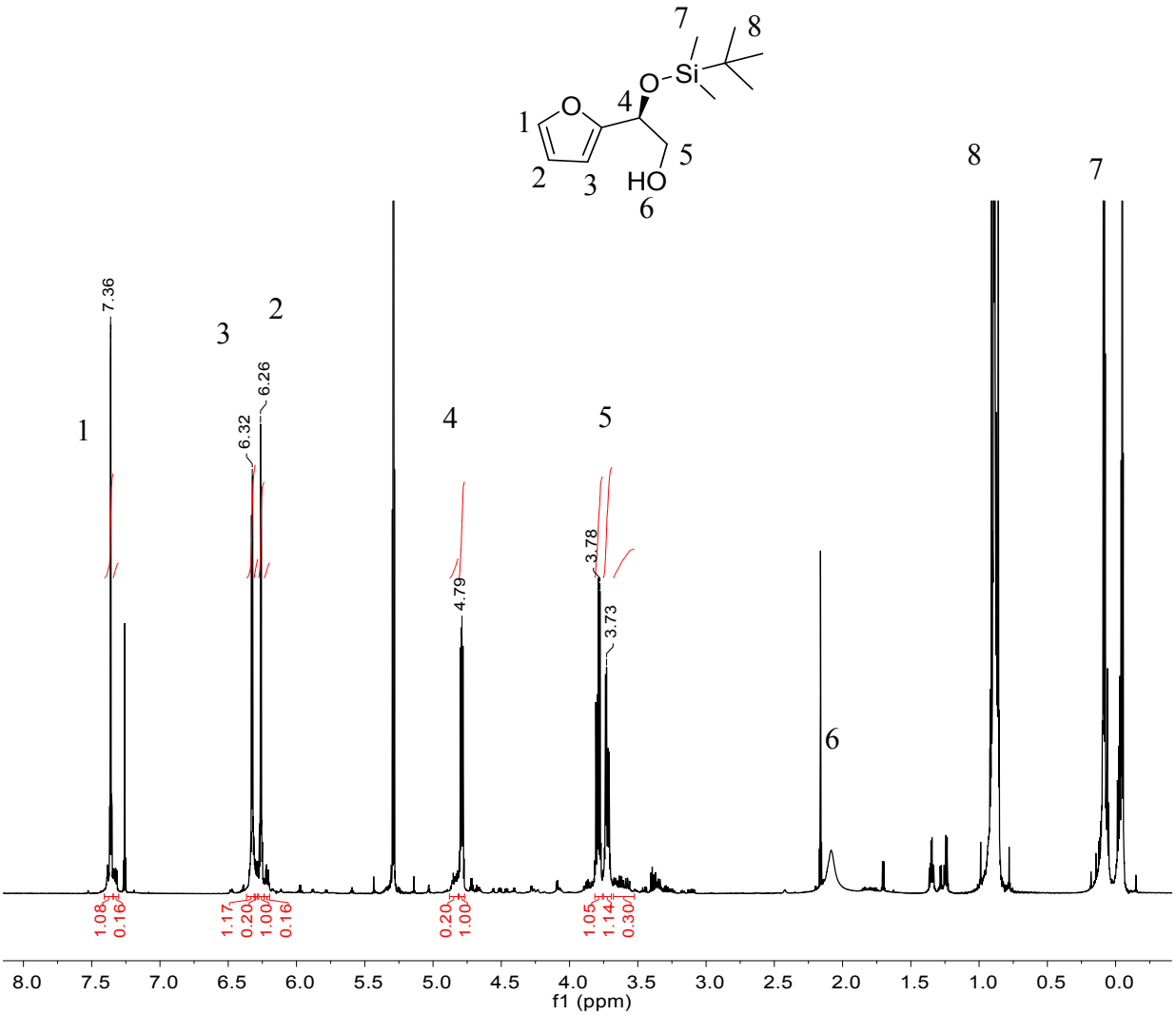

Figure S17: ^{1}H NMR of crude product after homopolymerization of **3** using photo-initiated RAFT polymerization as detailed in the main text, illustrating near quantitative conversion to **5** (600 MHz, $CDCl_3$, 25 °C). This NMR is nearly identical to that obtained from polymerization attempts using traditional living conditions with Lewis acids

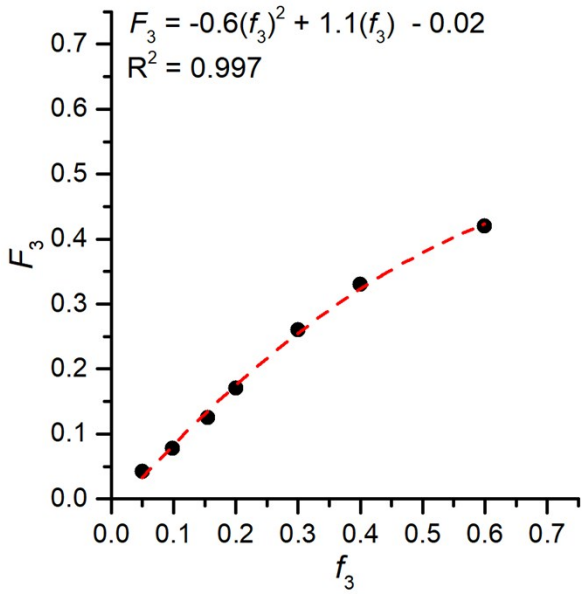

Figure S18: Plot of incorporation of **3** in the copolymer (F_3) vs molar feed ratio of **3** (f_3) showing the incomplete incorporation of **3** into the polymer compared to what was in the feed

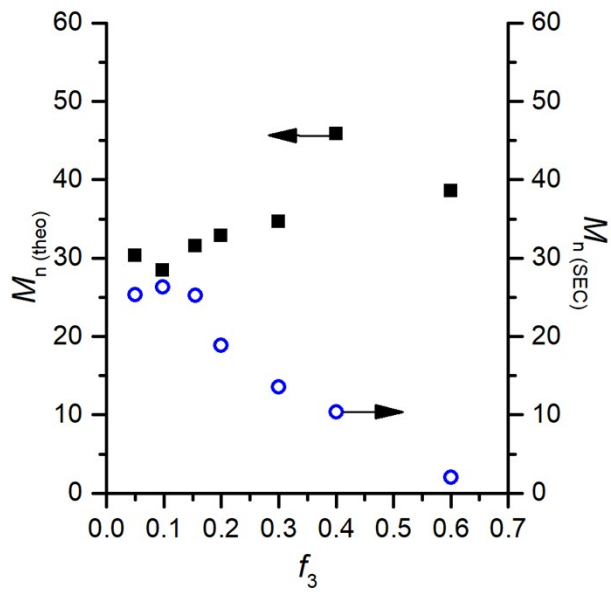

Figure S19: Plot of theoretical number average molar mass, $M_{n\ (theo)}$ (left y-axis, filled squares) compared to experimentally determined number average molar mass, $M_{n\ (SEC)}$ obtained from SEC analysis (right y-axis, open circles) for the copolymers as a function of feed ratio f_3

Table S1: Table of duplicate polarimetry experiments on copolymers with different molar fraction of **3** (F_3) along with the calculated weight fraction of **3** (w_3), specific optical rotation of the copolymers [α], and specific optical rotations normalized to w_3 $[\alpha]_{P3} = [\alpha] \times w_3$.

Sample	w_3	$[\alpha]_{589}^{25}$ (° mL g^{-1} dm^{-1})	c (mg mL^{-1})	c (P3) (mg mL^{-1})	$[\alpha]_{589}^{25}(P3)$ (° mL g^{-1} dm^{-1})
P4	0.096	-18.39	9.95	0.96	-191.52
		-17.74	9.55	0.92	-184.80
P8	0.170	-23.67	10.65	1.81	-139.29
		-31.68	7.55	1.28	-186.44
P13	0.257	-36.27	10.25	2.63	-141.20
		-35.93	12.05	3.10	-139.85
P17	0.331	-51.47	11.60	3.84	-155.32
		-55.40	9.05	3.00	-167.18
P26	0.460	-71.78	11.44	5.26	-156.22
		-74.15	10.12	4.66	-161.37
P33	0.544	-76.28	11.1	6.04	-140.27
		-75.57	15.6	8.49	-138.98
AVERAGE	-	-	-	-	-159
Std Dev	-	-	-	-	20

Equation S1: Calculation of weight fraction of **3** (w_3) from mol fraction in the polymer (F) and repeat unit molecular weight (M)

$$w_3 = \frac{F_3 M_3}{F_3 M_3 + F_{IBVE} M_{IBVE}}$$

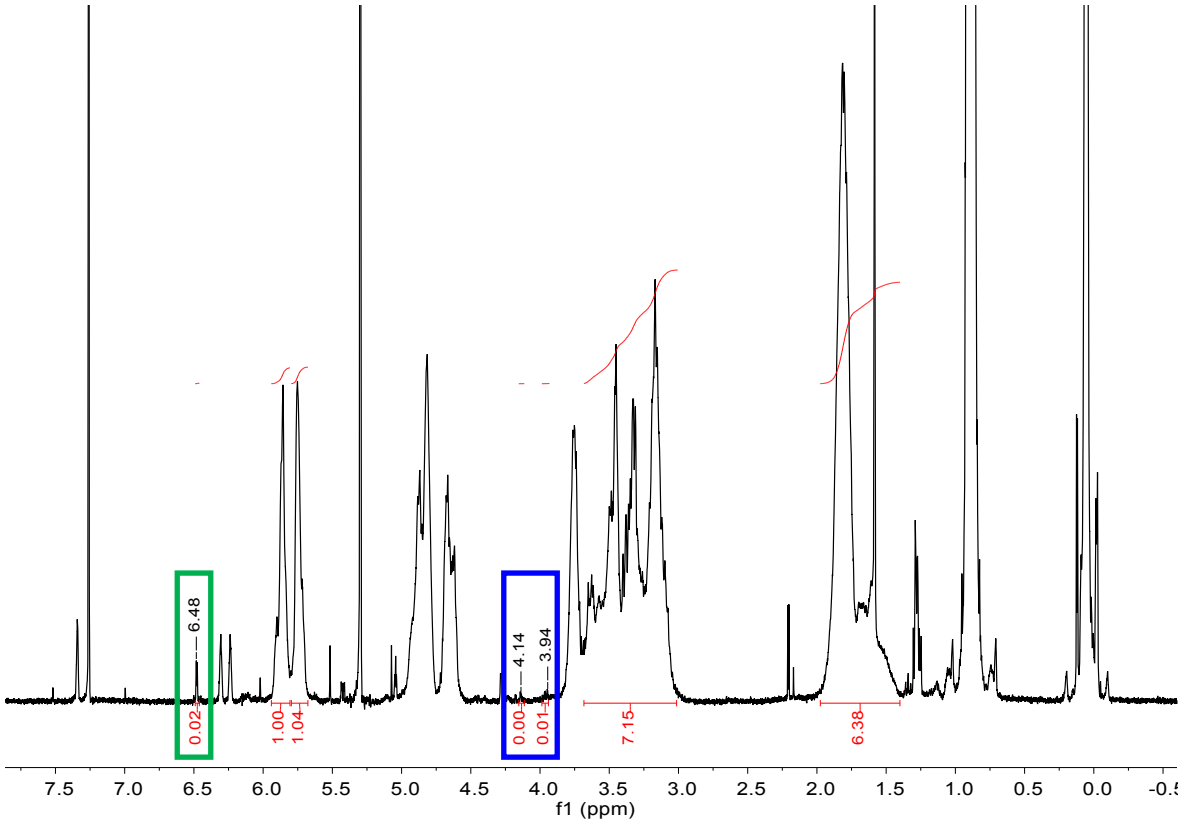

Figure S20: ^{1}H NMR of crude aliquot of P33 indicating near complete conversion for IBVE (distinct monomer peaks in blue box at δ ~ 4.14 and 3.94 ppm) as well as for THFF-TBDMS (monomer peak in green box δ ~ 6.48 ppm) (400 MHz, $CDCl_3$, 25 °C)

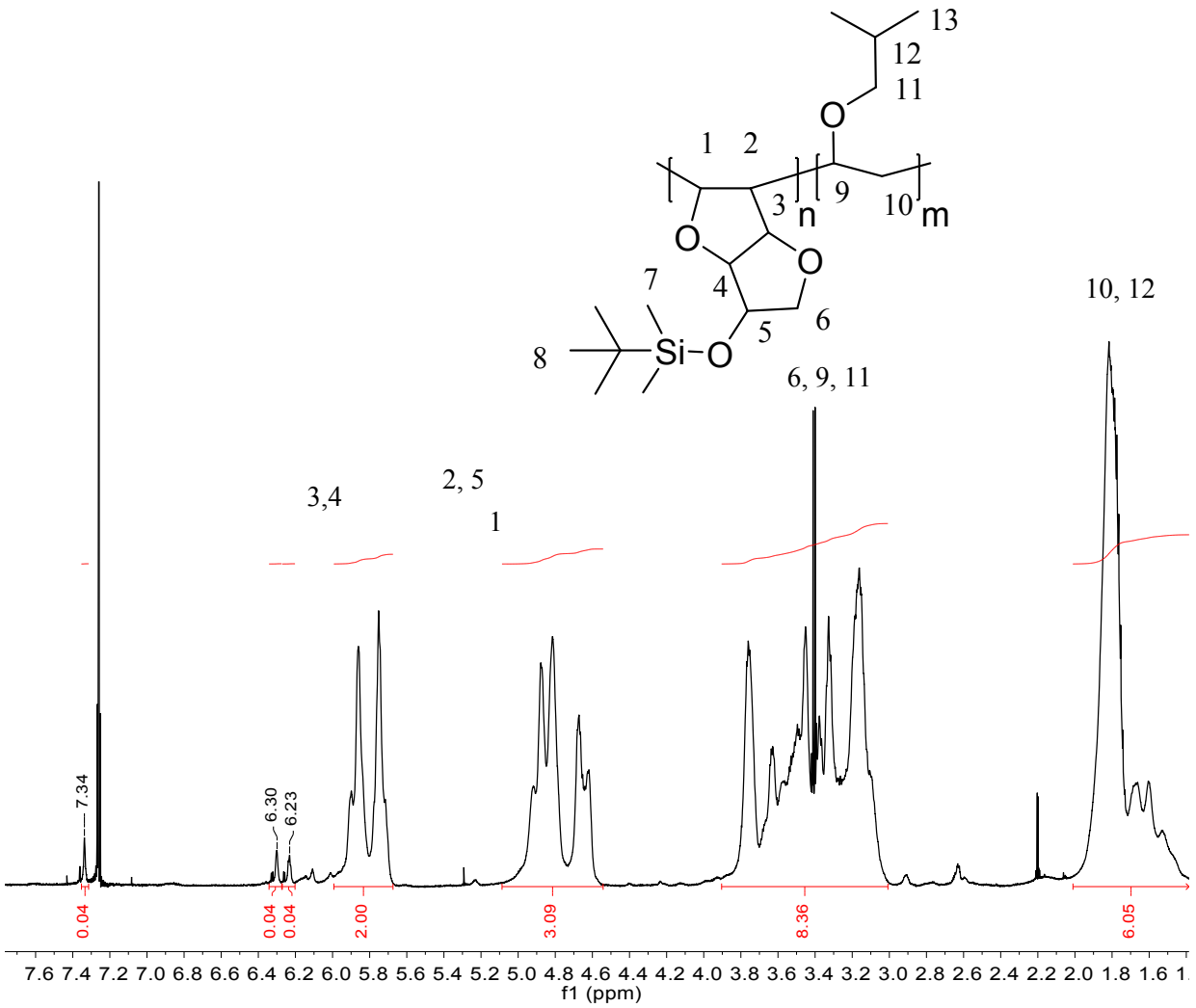

Figure S21: ^{1}H NMR of P33 showing presence of furanyl peaks post-precipitation (600 MHz, $CDCl_3$, 25 °C)

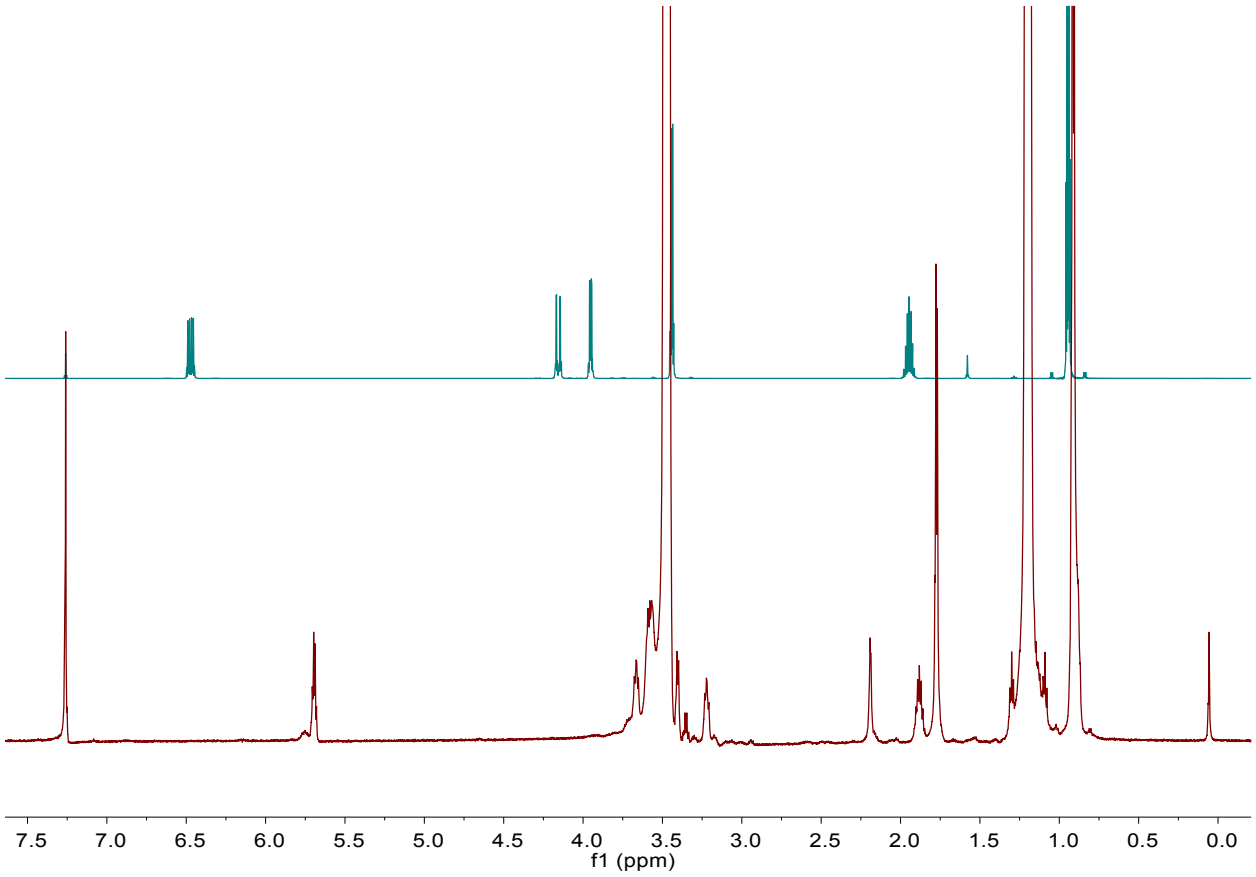

Figure S22: ^{1}H NMR of IBVE (top) and IBVE-HCl adduct (bottom) (600 MHz, $CDCl_3$)

Scheme S3: Synthesis of tetrahydrofuran-2-yl acetate (**6**) initiator

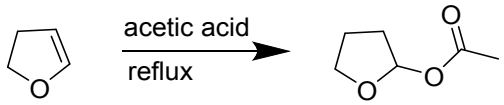

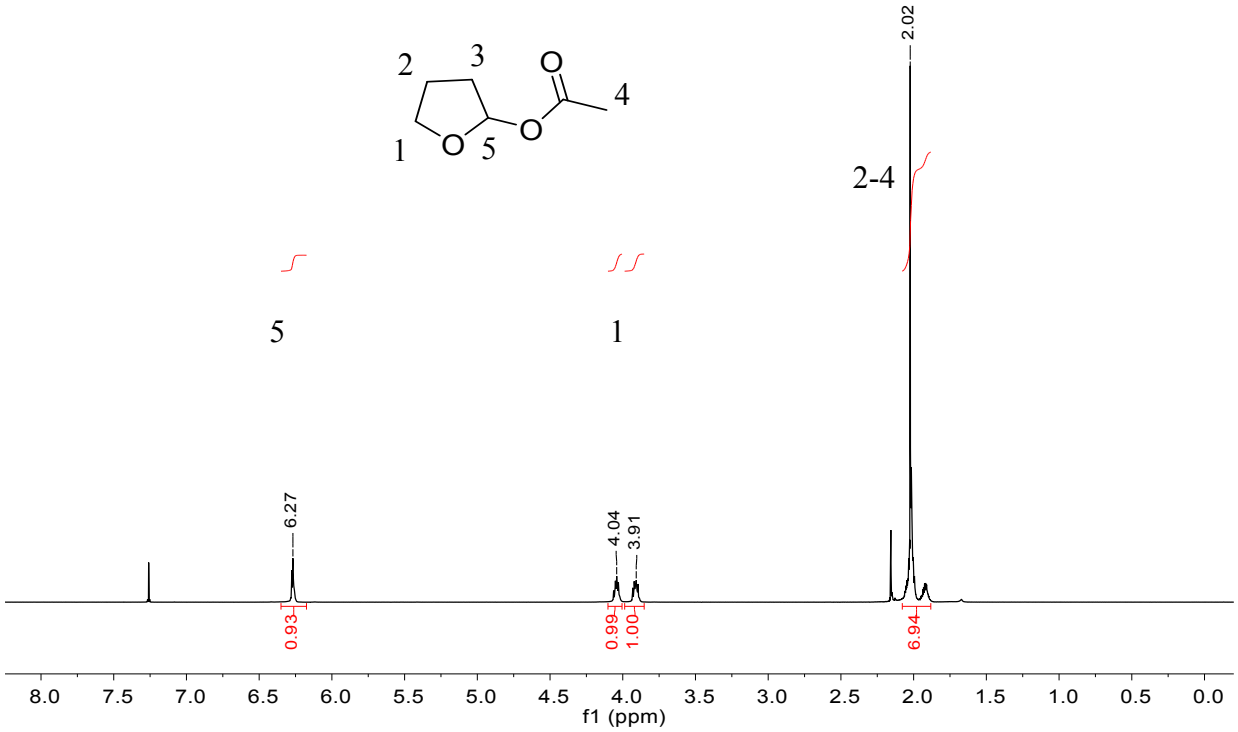

Figure S23: ^{1}H NMR of THFA (600 MHz, $CDCl_3$, 25 °C)

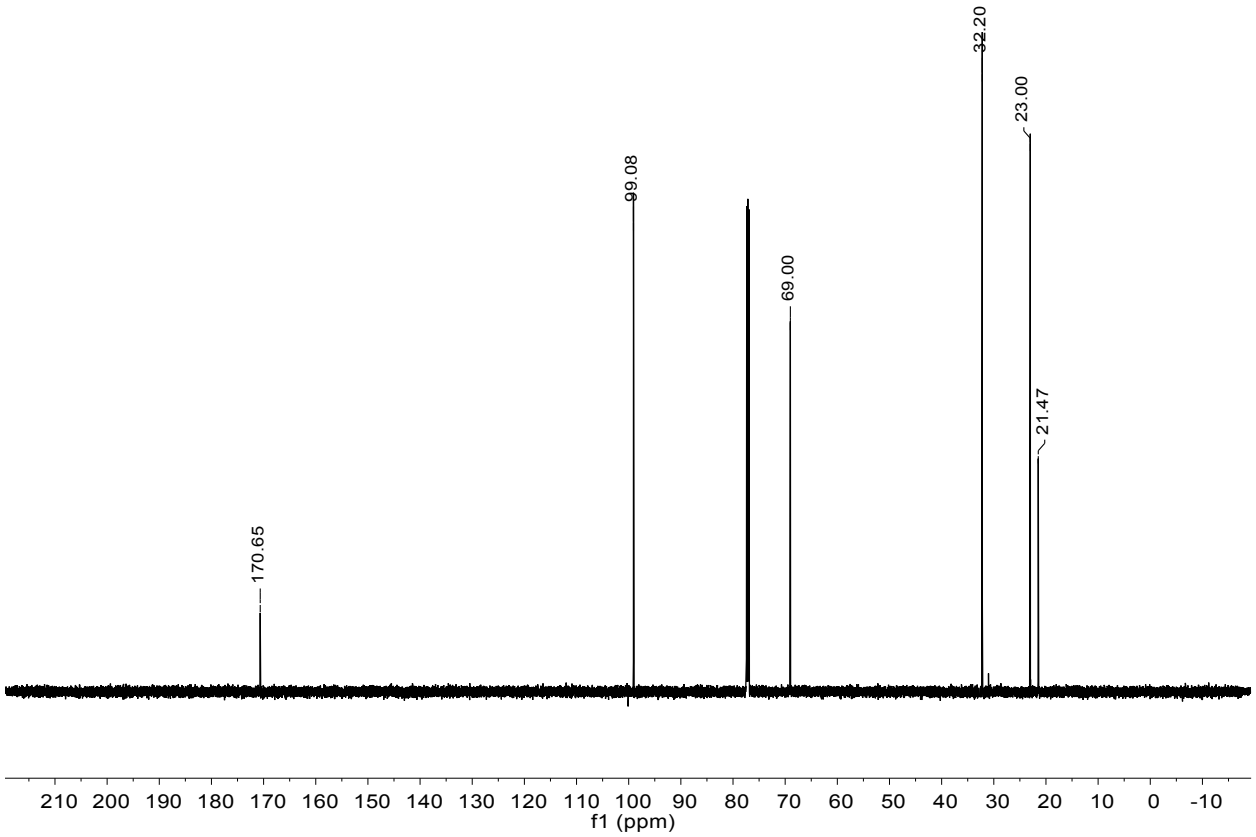

Figure S24: ^{13}C NMR of THFA (600 MHz, $CDCl_3$, 25 °C)

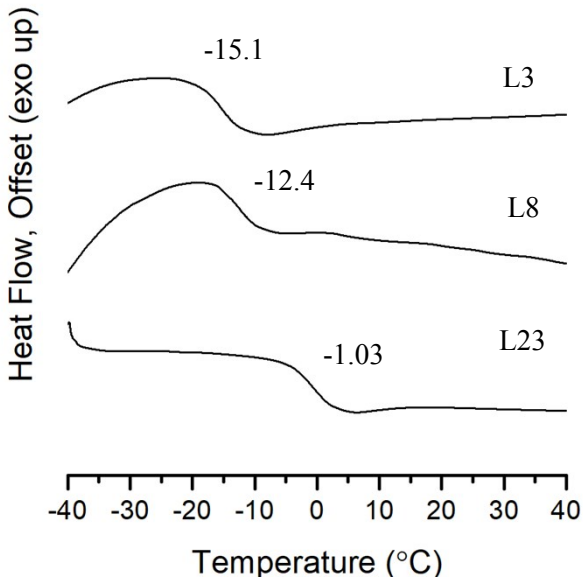

Figure S25: DSC thermogram of polymers (exo up) synthesized from traditional cationic methods, with F_3 increasing down the graph. Polymers were heated from -60 °C to 100 °C at a rate of 10 °C min^{-1}. Data was obtained from the third heat

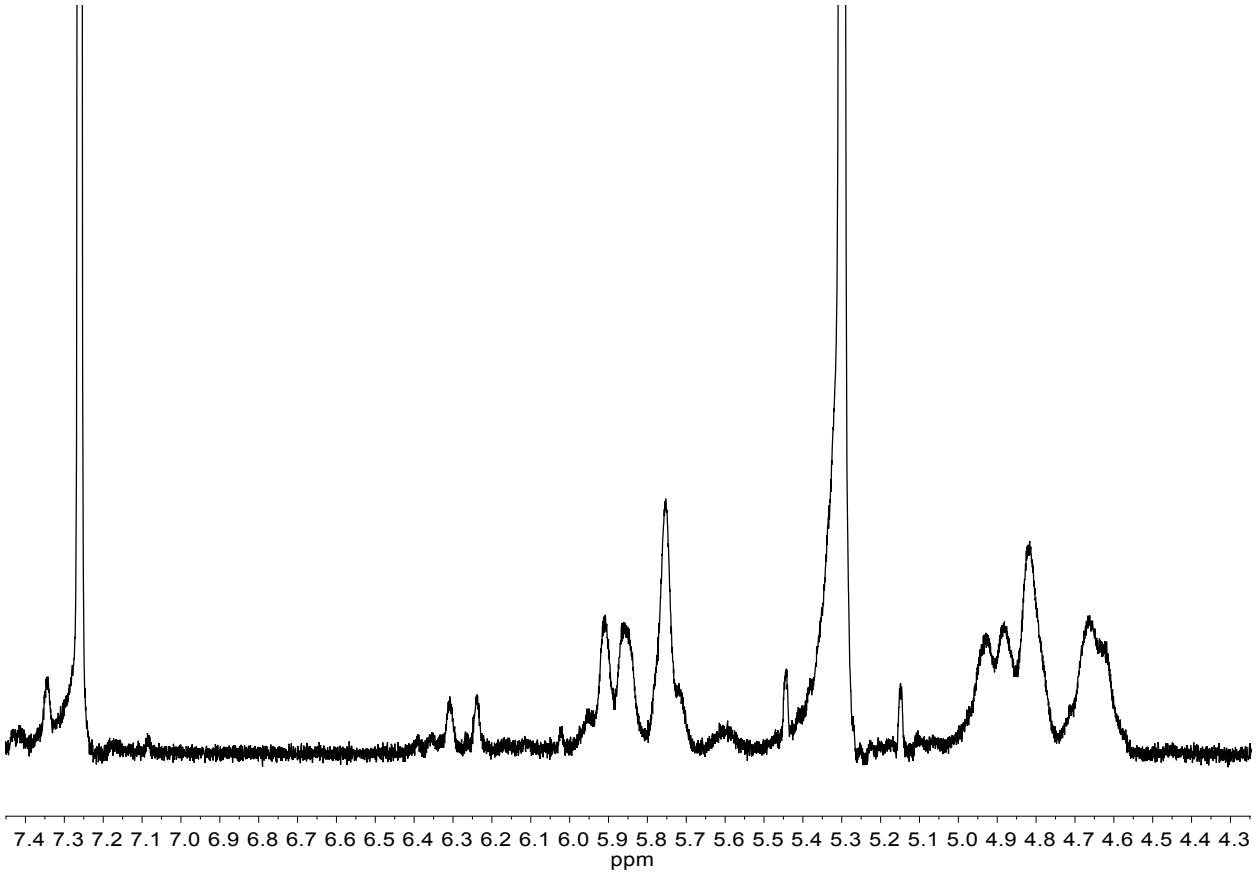

Figure S26: ^{1}H NMR of L8 zoomed in on the furanyl region, showing clear appearance of significant portions of **5** as well as the CTA after aqueous workup (before precipitation). Large peak ~5.3 ppm is DCM not completely removed via rotary evaporation (600 MHz, $CDCl_3$, 25 °C).

1. Berini, C.; Lavergne, A.; Molinier, V.; Capet, F.; Deniau, E.; Aubry, J. M., Iodoetherification of Isosorbide-Derived Glycals: Access to a Variety of O-Alkyl or O-Aryl Isosorbide Derivatives. *Eur. J. Org. Chem.* **2013,** *2013* (10), 1937-1949.
2. Paolucci, C.; Rosini, G., Approach to a better understanding and modeling of (S)-dihydrofuran-2-yl, (S)-tetrahydrofuran-2-yl-, and furan-2-yl-β-dialkylaminoethanol ligands for enantioselective alkylation. *Tetrahedron: Asymmetry* **2007,** *18* (24), 2923-2946.